HHS Public Access

Author manuscript

*NMR Biomed*. Author manuscript; available in PMC 2016 June 01.

Published in final edited form as:

*NMR Biomed*. 2015 June ; 28(6): 679–684. doi:10.1002/nbm.3308.

# Interventional MRI-Guided Local Delivery of Agents into Swine Bile Duct Walls Using MR Compatible Needle-Integrated Balloon Catheter System

**Feng Zhang, MD, PhD**, **Zhibin Bai, MD, PhD**, **Yaoping Shi, MD, PhD**, **Jianfeng Wang, MD, PhD**, **Yonggang Li, MD, PhD**, and **Xiaoming Yang, MD, PhD***

Image-Guided Bio-Molecular Intervention Research and Section of Vascular & Interventional Radiology, Department of Radiology; Institute for Stem Cell and Regenerative Medicine; University of Washington School of Medicine; 850 Republican Street, Seattle, WA, USA 98109

## Abstract

**Purpose—**To investigate the feasibility of interventional magnetic resonance imaging (MRI)-guided local agent delivery into pig common bile duct (CBD) walls using a newly-designed MR-compatible, needle-integrated balloon catheter system.

**Materials and Methods—**We first designed a needle-integrated balloon catheter system that is comprised of a 22-G MR-compatible Chiba biopsy needle and a conventional 12mm×2cm balloon catheter. Under fluoroscopy guidance, a custom needle/balloon system was positioned into the target CBD via a transcholecystic access. T1-weighted MR imaging was used to localize and reposition the needle/balloon system in the target. A 0.5-mL mixture of motexafin gadolinium (MGd) and trypan blue dye as well as 5-fluorouracil (5-Fu) was delivered into the CBD wall through the needle/balloon system. Post-infusion T1-weighted MR imaging was obtained and contrast-to-noise ratios (CNR) of CBD walls of pre- and post-MGd/blue infusions were compared by a paired t-test. In addition, post-infusion x-ray cholangiography was achieved to evaluate the potential injuries of CBDs by the needle/balloon system. Subsequent histologic analysis was performed to correlate and confirm the imaging findings.

**Results—**Post-infusion cholangiogram didn't show any extravasation of contrast agent, indicating no procedure-related damage to the CBDs. MR imaging demonstrated the clear enhancement of the target bile duct walls infused with MGd/trypan blue dye with average penetration depth of 4.7±1.2mm. The average CNR of the post-infusion bile ducts was significant higher than that of the pre-infusion bile ducts (110.6±22 vs 5.7±2.8, $p<0.0001$). Histology depicted the blue dye staining and red fluorescence of MGd through the target CBD walls, which was well correlated with the imaging findings.

**Conclusions—**It is feasible to use the new MR compatible, needle-integrated balloon catheter system for intrabiliary local agent delivery into CBD walls under MR imaging guidance, which may open new avenues for efficient management of pancreatobiliary malignancies using MR-guided interventional oncology.

*Correspondence to: Xiaoming Yang, MD, PhD, Image-Guided Bio-Molecular Intervention Section, Department of Radiology, University of Washington School of Medicine, 850 Republican Street, S470, Seattle, Washington, USA., Phone: 206-685-6967, Fax: 206-221-0647, xmyang@u.washington.edu.

## Graphical abstract

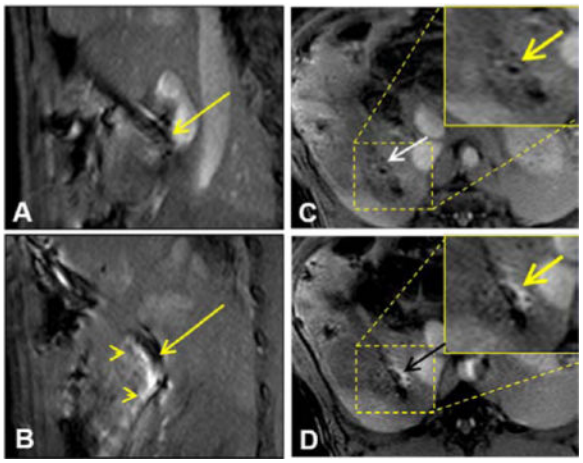


## Introduction

Pancreatobiliary cancer remains one of the deadliest malignant diseases worldwide. Approximately 9,000 new cases of biliary cancer and 46,000 cases of pancreatic cancer are diagnosed in the United States (1,2). Due to the lack of early symptoms and the tendency of the tumor to invade surrounding structures or metastasize at an early stage, most patients have advanced disease at the time of their diagnosis. The five-year survival rate is less than 5%. Although surgical resection offers the only potential chance of cure for patients with pancreatobiliary cancers (1–3), unfortunately, very few patients have the chance to receive the surgery treatment due to the advanced stage of the disease with pervasive metastasis at the presentation (3–5). In current clinical practice, the only direct treatment for pancreatobiliary tumors involves systemic chemotherapy with or without radiation therapy. However, the benefits of systemic chemotherapy are limited by its non-specific delivery, which results in low drug doses at the targeted malignant biliary regions and systemic toxicities to other organs (5–7).

MR Imaging-guided minimally-invasive interventional technology permits local delivery of high-dose drug to target tissues, which thus overcome the key drawback of systemic chemotherapeutic drug administration – toxicity to other vital organs. Recent efforts have been made to develop an intrabiliary local agent delivery approach, which may enable one to instantly monitor and evaluate the chemotherapeutic drug delivery efficacy of intrabiliary local agent delivery under magnetic resonance imaging (MRI)(8,9). This new technique involved the use of a multiporous balloon catheter that was percutaneously placed into the common bile duct (CBD), where chemotherapeutic drugs were locally infused into CBD walls (8,9). However, the infusion capability of the multiporous balloon has limited penetration depth of agents into the bile duct wall, and thereby deposits only limited amount of chemotherapeutic drugs at the target bile duct (8). This characteristics of the multiporous balloon is certainly not suitable for intrabiliary treatment of the pancreatic head cancer, which, unlike biliary cancer growing along the bile duce wall, compresses and obstructs the distal CBD by a mass growing outside of the biliary tract. To solve this problem, we

attempted to develop a technique of interventional MRI-guided local delivery of sufficient dose of agents into deep-seated targets using an intrabiliary needle-integrated balloon catheter system.

## Materials and Methods

### Design of the MR-compatible intrabiliary needle-integrated balloon catheter system

The needle-integrated balloon catheter system was comprised of a 22-G MR compatible Chiba biopsy needle (MReye Disposable Chiba Biopsy Needle, Cook Inc. IN) and a conventional 12mm×2cm balloon catheter (Charger, Boston Scientific, Natick, MA). The 3-mm-long, 150°-curved tip of a 22G MR-compatible biopsy needle was restrained on the surface of the balloon and oriented perpendicular to the long axis of the catheter. The deflated balloon provided a protective covering of the curved needle tip, which ensured a smooth pass through the bile duct via a percutaneous access. Once the needle/balloon system was positioned into the target bile duct segment, the puncture direction of the curved needle tip could be adjusted towards the target (such as a pancreatic head tumor mass). Subsequent full inflation of the balloon with saline can push the needle tip through the bile duct wall into the deep-seated target, to which high-dose agent could be injected (Figure 1). The system can be fit into a 10 or 11 French sheath, which is placed in the common bile duct through a transcholecystic approach. With application of a vacuum, the balloon deflates, and the needle is retracted for removal of the device from the bile duct lumen.

### Animal experiments

**Animals—**Pig experiments were approved by the Institutional Animal Care and Use Committee. Eight domestic pigs, 50–60 Kg in weight, were sedated by intramuscular injection of Telazol at 4.4mg/kg body weight and Xylazine at 1mg/kg body weight, and then mechanically ventilated with 1%-3% isoflurane in 100% oxygen.

**Catheterization of common bile ducts (CBDs)—**A subcostal incision was made to expose the gallbladder. The gallbladder was mobilized and raised out of the peritoneal cavity. Under fluoroscopic guidance, an 11 French sheath (SafeSheath® Ultra, Pressure Products, CA) was advanced, through the gallbladder and the cystic duct, into the CBD over a 0.035-inch hydrophilic guidewire (Terumo Corporation, Tokyo, Japan). Over the guidewire, we placed the intrabiliary needle/balloon system into the distal portion of CBD (Figure 2A). Then, we closed the abdominal incision in layers using interrupted non-absorbable sutures on the peritoneum, muscles and skin. The introducer was secured to the skin.

**Intrabiliary chemotherapeutic drugs delivery—**Each animal was placed supine on the 3.0T MR scanner table (Philips Healthcare, Best, the Netherlands). We acquired axial, sagittal and coronal fat-suppressed and respiration-gated T1 weighted images of bile duct walls and the needle/balloon system, using a Torso phase-array surface coil. Based on these MR images, we adjusted the position of the needle/balloon to the target bile duct, and then inflated the needle-integrated balloon with 1% MultiHance (Bracco Diagonostics Inc, Princeton,NJ). Pre-injection MR imaging was performed with a turbo field echo sequence

(TFE) using 10/1-msec TR/TE, 300-mm FOV, 15°flip angle, 3-mm slice thickness, 320×320 matrix, and 4 NEX. Subsequently, through the needle channel, a 0.5-mL mixture solution, containing 5mg 5-fluorouracil (5-Fu), 125ug motexafin gadolinium (MGd) and trypan blue dye, was injected into the CBD wall. Here trypan blue dye was used for subsequent histology analysis to confirm the penetration and distribution of agent in the bile duct wall and surrounding tissue. Thus, as a T1 weighted MR contrast agent and red fluorescence emitter, MGd was used for both instant MR imaging monitoring and subsequent histology confirmation by confocal microscopy. Immediately after agent administration, axial, sagittal and coronal fat-suppressed and respiration-gated T1 weighted MR images of bile duct walls were acquired, using the same parameters as described for pre-injection MRI. After MRI, the animals were transported back to the surgery-fluoroscopy lab, where post-infusion cholangiogram was obtained to see any potential rupture of the injected CBDs by the new needle/balloon system.

**Imaging analysis—**We measured signal intensities (SIs) of the CBD walls and the peri-CBD tissues where the solution of 5-FU and MGd as well as trypan blue was injected. We calculated the average contrast-to-noise ratio (CNR) by using the following equation: $(SI_{CBD}-SI_{peri\text{-}CBD})$/SD noise, where SD noise is the standard deviation of the background noise. The 1-$mm^2$ region of interest was placed by one experienced radiologist. The penetration depth of MGd (starting from inner bile duct wall) in the bile duct wall and surrounding tissue was measured as well.

## Histology

Immediately after MR imaging, each animal was euthanized. The MGd/trypan blue–infused CBD segment or un-infused CBD segment (as a control) was harvested for histologic correlation to confirm the successful penetration of MGd/trypan blue into the CBD wall. We used optical imaging, at excitation wavelength of 470nm and emission wavelength of 750nm, to display MGd-emitting red fluorescence in the bile duct tissue. The small segments of bile ducts were cryosectioned at 8 μm and then examined by using laser confocal microscopy to detect red fluorescence of MGd.

## Drug Quantification

For 5-Fu quantification in bile duct tissues, drug-delivered CBDs were harvested and homogenized in 5mL PBS using a tissue grinder (PYREX Ten Broeck, Corning, NY). After centrifuging the suspension at 3000 rpm for 10mins, we extracted 5-Fu by adding 2 ml of isopropyl alcohol and 5 ml ethyl acetate to 0.5 ml samples; the suspension was vortexed, centrifuged for 10 min at 3,000 rpm. The supernatant was then transferred to another tube and dried under a gentle stream of nitrogen flow. The dried samples were reconstituted in 200 μl mobile phase (water/methanol: 90/10) and analyzed using high-pressure liquid chromatography (HPLC) (Waters, Milford, MA), by using our established protocol. The linear regression analysis was performed by plotting the peak areas (y) of the drug against the respective concentration (x).

### Statistical analysis

Statistical software (SPSS, version 19.0; SPSS Chicago, Ill) was used for all data analysis. Paired *t*-test was used to compare the CNRs of the bile ducts with MRI between pre- and post-injection of the mixed solution into the CBD walls.

## Results

In all animals, intrabiliary injections of MGd and trypan blue dye were successfully performed. Post-infusion cholangiogram didn't show any extravasation of X-ray contrast agent, which indicates no needle puncture-related injury of the drug-injected bile duct walls (Figure 2B).

The needle-integrated balloon catheter used in this study could be clearly visualized on T1WIs as a dark structure in the CBD lumen, even though there was some artifact arising from the needle tip (Figure 3A&B). These imaging features facilitated guidance of the needle/catheter in the bile duct, confirmation of the position of the needle tip, and the adjusting of puncture direction of the needle tip into the bile duct tissue. Following the needle puncture into the bile duct wall driven by the inflated balloon, MGd was successfully injected into the bile duct walls and surrounding tissues, demonstrated as a clearly bright region extending from the needle tip into the bile duct wall and adjacent tissue (Figure 3C&D). We achieved an average penetration depth of 4.7±1.2mm and an average MGd perfusion length of 21±1.5mm in the bile ducts and their surrounding tissues. Intrabiliary post-injection of MGd caused a significant increase in regional signal intensity compared with that of the pre-infusion on T1W MR Images. The average CNR of the post-infusion bile ducts was significantly higher than that of the pre-injection bile ducts (110.6±22 vs 5.7±2.8, $p<0.0001$).

We harvested the entire bile duct and surrounding tissue including the hepatoduodenal ligament and portion of duodenum and pancreas for ex-vivo optical imaging. Optical imaging showed the MGd infiltration in the bile duct wall and adjacent tissue, manifesting as bright red fluorescence in the MGd-injected region (Figure 4A), which was correlated with the blue dye staining in the same region (Figure 4B). Confocal microscopy further confirmed MGd penetration through the bile duct wall and surrounding tissue, featuring as red fluorescent dots in the cells and extracellular space, which was not seen in the control bile duct without the injection of MGd and trypan blue dye (Figure 4C&D).

We plotted the peak areas (y) of the chemotherapeutic drug against its respective concentration (x). Regression correlation coefficients of the lineal curve were above 0.990. Quantitative analysis of 5-FU by HPLC showed that out of the total 5mg 5-FU injected into the bile duct tissue, 4.1±0.12 mg 5-FU were retrieved, proving an approximately 80% drug delivery efficiency.

## Discussion

Pancreatic adenocarcinoma and cholangiocarcinoma are hypovascular and fibrosis-rich tumors, which make systemic chemotherapy less effective. The technique of intrabiliary MR

imaging-guided delivery of high-dose therapeutic agents into tumor masses had been developed in previous studies with an attempt to overcome the barrier, that limited amount of drugs is delivered into the tumor cells, through a systemic administration route (8,9). The quantities of chemotherapeutic drugs delivered into the bile duct tissue through a multiparous balloon were less than 1 mg per gram of bile duct tissue, which means the potential of translating this technique to clinical application is suboptimal (8). To date, several balloon catheter-based intraluminal agent delivery techniques have been developed for locally administering therapeutics into vascular targets, such as passive diffusion by applying a double-occlusion balloon, pressure driven infusion by a balloon with multiple micropores, and mechanically or electrically enhanced delivery (10). The texture of pancreatobiliary cancers is very hard due to marked fibrosis and stromal myofibroblasts, which doesn't allow high dose of therapeutic agents entering the tumor tissues via the capabilities of passive diffusion or pressure driven infusion approaches. We developed a MR compatible needle-integrated balloon system. The advantage of this needle/balloon system is that it can be used to deliver drugs into tumors via a mechanical penetration mode with a sufficient deep infiltration of delivered agents into the targets.

The results of our study have validated the feasibility of using the newly-designed MR compatible, needle-integrated balloon catheter system to locally deliver high dose agent into the deep-seated target of common bile duct, which can be accurately guided by clinical 3.0T MR imaging. Interventional MR imaging is a valuable tool to monitor the penetration and distribution of MGd and 5-FU into CBD walls with significantly increased penetration depth and chemotherapeutic drug dosage in the biliary tissue. Thus, this technical development may specifically pose great value for locally treating pancreatic head adenocarcinoma by local administrating high quantity of therapeutic agents into the tumor masses using this new needle/balloon catheter system.

MRI has been used to guide interventions and cancer biopsies (11–15). The advantages of MR imaging include 3D steering of the imaging plane, excellent soft tissue contrast, elimination of iodinated contrast agents, and no risk of ionizing radiation. During MRI-guided intervention, high-resolution anatomic and functional imaging can be performed to quantify the delivered agent within the target tissues (13,14,16,17). Interventional MR imaging technique can accurately guide the deployment of the needle/balloon system in the bile duct lumen, and allow the instant visualization of the needle puncture in the target. Our study demonstrates the potential of using this technique to treat pancreatobiliary cancers, and then may immediately assess the infiltration scope and penetration depth of therapeutic agents in the tumor target. MR imaging can help us to not only validate the drug delivery efficiency but also to evaluate the tumor status regarding tumor size and staging once this technique can be translated into the clinical application. When the needle/balloon system is deployed in the tumor region, we can precisely adjust the needle/balloon system according to the information acquired from MR images of the tumors, and thereby achieve the effective drug delivery. We used MGd as the bio-imaging marker for evaluating the efficacy of this interventional MRI-guided agent delivery technique. MGd has multifunctional features: (i) a chemotherapeutic agent for treating cancer (18); (ii) an intracellular T1 MRI contrast agent for specifically indicating the successful delivery of drugs into the target tumor (19); (iii) an emitter of red-colored fluorescence for confirming the drug delivery by

subsequent histology examination; and (iv) a sensitizer to radiation therapy (20). Recent study reported that the intracellular internalization of MGd by cancer cells was in a concentration-dependent manner, which encouraged us to develop interventional molecular MR imaging technique to guide the treatment of panceatobiliary cancers (9).

This study primarily focused on the design and development of the new MR-compatible, needle-integrated balloon system. It is highly valuable to test this new device and technique on a large animal model such as a swine model with pancreatic cancers or bile duct cancer. However, it is unfortunate that no large animal models with pancreatic cancers or bile duct cancers are available around the world. It is warranted to further perform comprehensive studies using survival animals to evaluate the safety and long-term impact of this new technique on treatment of pancreatobiliary malignancies.

In conclusion, it is feasible to use the new MR compatible, needle-integrated balloon catheter system for intrabiliary local agent delivery into CBD walls under MR imaging guidance, which may open new avenues for efficient management of pancreatobiliary malignancies using MR-guided interventional oncology.

## Acknowledgments

Founding support: This study was supported by an NIH RO1EBO12467 grant.

## Abbreviations

| | |
|---|---|
| **MGd** | motexafin gadolinium |
| **MRI** | magnetic resonance imaging |
| **CBD** | common bile duct |
| **TFE** | turbo field echo |
| **5-Fu** | 5-fluorouracil |
| **T1WI** | T1 weighted imaging |
| **SIs** | signal intensities |
| **CNR** | contrast-to-noise ratio |
| **HPLC** | high-pressure liquid chromatography |

## References

1. Ryan DP, Hong TS, Bardeesy N. Pancreatic adenocarcinoma. The New England journal of medicine. 2014; 371(11):1039–1049. [PubMed: 25207767]
2. Valle J, Wasan H, Palmer DH, Cunningham D, Anthoney A, Maraveyas A, Madhusudan S, Iveson T, Hughes S, Pereira SP, Roughton M, Bridgewater J, Investigators ABCT. Cisplatin plus gemcitabine versus gemcitabine for biliary tract cancer. The New England journal of medicine. 2010; 362(14):1273–1281. [PubMed: 20375404]
3. Jemal A, Siegel R, Ward E, Hao Y, Xu J, Murray T, Thun MJ. Cancer statistics, 2008. CA: a cancer journal for clinicians. 2008; 58(2):71–96. [PubMed: 18287387]

4. Hidalgo M. Pancreatic cancer. The New England journal of medicine. 2010; 362(17):1605–1617. [PubMed: 20427809]
5. Tonini G, Virzi V, Fratto ME, Vincenzi B, Santini D. Targeted therapy in biliary tract cancer: 2009 update. Future Oncol. 2009; 5(10):1675–1684. [PubMed: 20001803]
6. Williams KJ, Picus J, Trinkhaus K, Fournier CC, Suresh R, James JS, Tan BR. Gemcitabine with carboplatin for advanced biliary tract cancers: a phase II single institution study. HPB: the official journal of the International Hepato Pancreato Biliary Association. 2010; 12(6):418–426. [PubMed: 20662793]
7. Wolfgang CL, Herman JM, Laheru DA, Klein AP, Erdek MA, Fishman EK, Hruban RH. Recent progress in pancreatic cancer. CA: a cancer journal for clinicians. 2013; 63(5):318–348. [PubMed: 23856911]
8. Zhang F, Le T, Wu X, Wang H, Zhang T, Meng Y, Wei B, Soriano SS, Willis P, Kolokythas O, Yang X. Intrabiliary RF heat-enhanced local chemotherapy of a cholangiocarcinoma cell line: monitoring with dual-modality imaging–preclinical study. Radiology. 2014; 270(2):400–408. [PubMed: 24471389]
9. Zhang F, Li J, Meng Y, Sun J, Soriano SS, Willis P, Gu H, Glickerman D, Yang X. Development of an intrabiliary MR imaging-monitored local agent delivery technique: a feasibility study in pigs. Radiology. 2012; 262(3):846–852. [PubMed: 22357886]
10. Yang X. Imaging of vascular gene therapy. Radiology. 2003; 228(1):36–49. [PubMed: 12738874]
11. Spuentrup E, Ruebben A, Schaeffter T, Manning WJ, Gunther RW, Buecker A. Magnetic resonance–guided coronary artery stent placement in a swine model. Circulation. 2002; 105(7): 874–879. [PubMed: 11854130]
12. Buecker A, Spuentrup E, Ruebben A, Mahnken A, Nguyen TH, Kinzel S, Gunther RW. New metallic MR stents for artifact-free coronary MR angiography: feasibility study in a swine model. Investigative radiology. 2004; 39(5):250–253. [PubMed: 15087718]
13. Tzifa A, Krombach GA, Kramer N, Kruger S, Schutte A, von Walter M, Schaeffter T, Qureshi S, Krasemann T, Rosenthal E, Schwartz CA, Varma G, Buhl A, Kohlmeier A, Bucker A, Gunther RW, Razavi R. Magnetic resonance-guided cardiac interventions using magnetic resonance-compatible devices: a preclinical study and first-in-man congenital interventions. Circulation Cardiovascular interventions. 2010; 3(6):585–592. [PubMed: 21098745]
14. Kuhn JP, Langner S, Hegenscheid K, Evert M, Kickhefel A, Hosten N, Puls R. Magnetic resonance-guided upper abdominal biopsies in a high-field wide-bore 3-T MRI system: feasibility, handling, and needle artefacts. European radiology. 2010; 20(10):2414–2421. [PubMed: 20503050]
15. Menard C, Iupati D, Publicover J, Lee J, Abed J, O'Leary G, Simeonov A, Foltz WD, Milosevic M, Catton C, Morton G, Bristow R, Bayley A, Atenafu EG, Evans AJ, Jaffray DA, Chung P, Brock KK, Haider MA. MR-guided Prostate Biopsy for Planning of Focal Salvage after Radiation Therapy. Radiology. 2014; 122681
16. Yang X, Atalar E, Li D, Serfaty JM, Wang D, Kumar A, Cheng L. Magnetic resonance imaging permits in vivo monitoring of catheter-based vascular gene delivery. Circulation. 2001; 104(14): 1588–1590. [PubMed: 11581132]
17. Krombach GA, Pfeffer JG, Kinzel S, Katoh M, Gunther RW, Buecker A. MR-guided percutaneous intramyocardial injection with an MR-compatible catheter: feasibility and changes in T1 values after injection of extracellular contrast medium in pigs. Radiology. 2005; 235(2):487–494. [PubMed: 15858090]
18. Miller RA, Woodburn KW, Fan Q, Lee I, Miles D, Duran G, Sikic B, Magda D. Motexafin gadolinium: a redox active drug that enhances the efficacy of bleomycin and doxorubicin. Clin Cancer Res. 2001; 7(10):3215–3221. [PubMed: 11595717]
19. De Stasio G, Rajesh D, Ford JM, Daniels MJ, Erhardt RJ, Frazer BH, Tyliszczak T, Gilles MK, Conhaim RL, Howard SP, Fowler JF, Esteve F, Mehta MP. Motexafin-gadolinium taken up in vitro by at least 90% of glioblastoma cell nuclei. Clin Cancer Res. 2006; 12(1):206–213. [PubMed: 16397044]

20. Madsen SJ, Mathews MS, Angell-Petersen E, Sun CH, Vo V, Sanchez R, Hirschberg H. Motexafin gadolinium enhances the efficacy of aminolevulinic acid mediated-photodynamic therapy in human glioma spheroids. J Neurooncol. 2009; 91(2):141–149. [PubMed: 18777009]

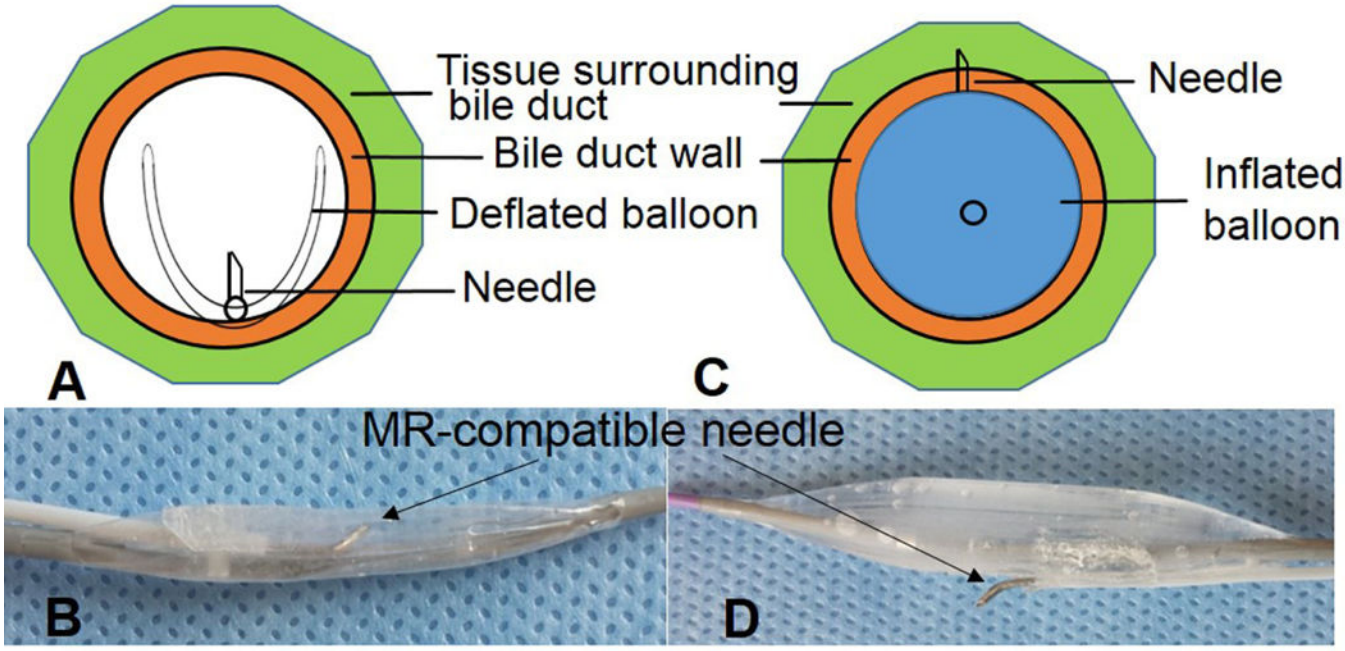


**Figure 1.**

Design of the intrabiliary agent delivery system, which is comprised of an MR-compatible needle and a balloon catheter. **(A&B)** The needle is attached onto the surface of the balloon. The deflated balloon provides a protective covering for the needle for smooth pass within the bile duct. **(C&D)** When the balloon is positioned in the target bile duct, a full inflation of the balloon pushes the needle to puncture the bile duct wall and surrounding tissue for deep agent delivery.

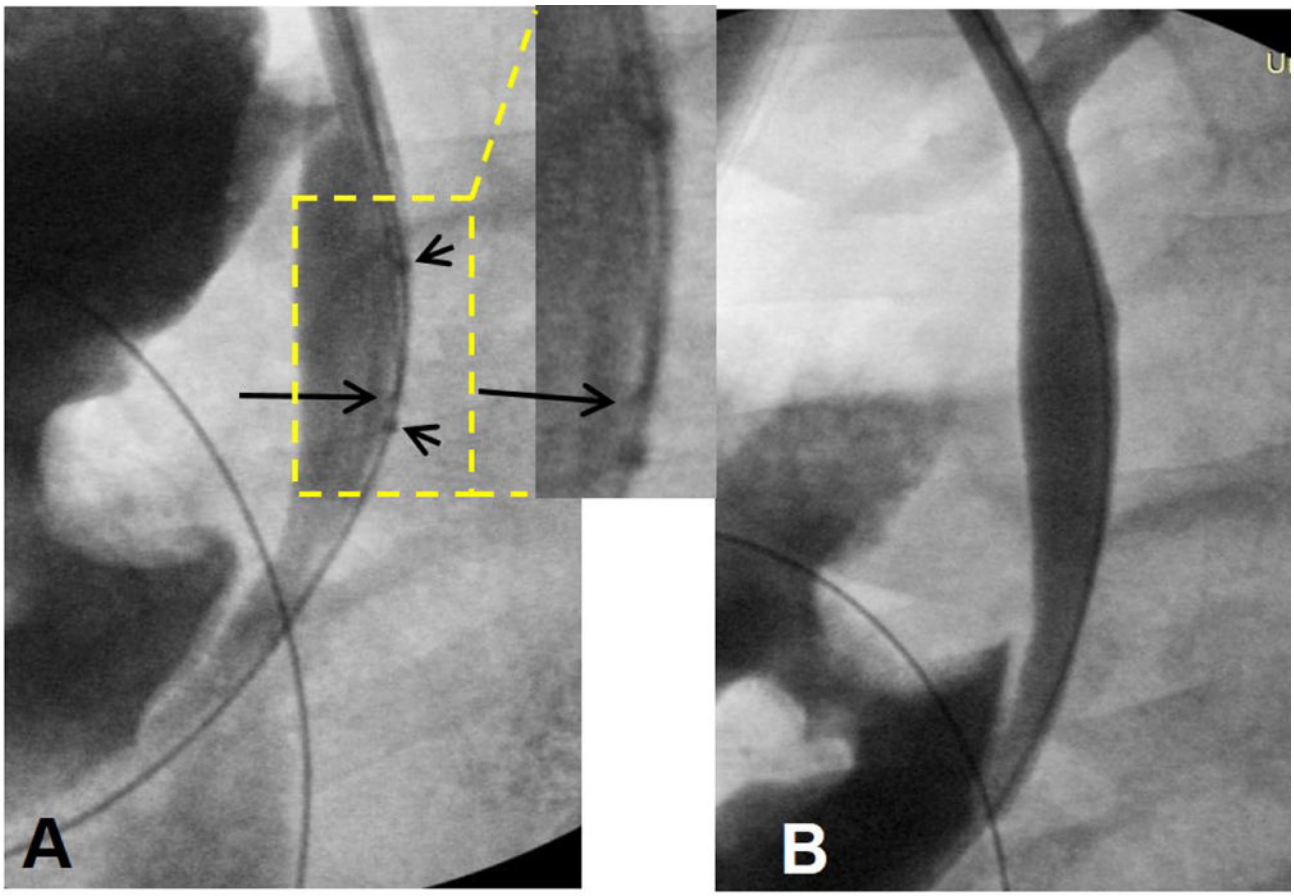


**Figure 2.**

Fluoroscopy-guided placement of needle-integrated balloon catheter system in a pig common bile duct (CBD). **(A)** Via a transcholecystic approach, the needle/balloon system is positioned into CBD through an 11Fr sheath, and then the needle tip direction is adjusted toward the bile duct wall (long arrow). Two short arrows indicate the markers of the balloon. **(B)** Post-injection cholangiography confirms the continuity of bile duct wall with no contrast extravasation, indicating no procedure-related damage to the bile duct wall.

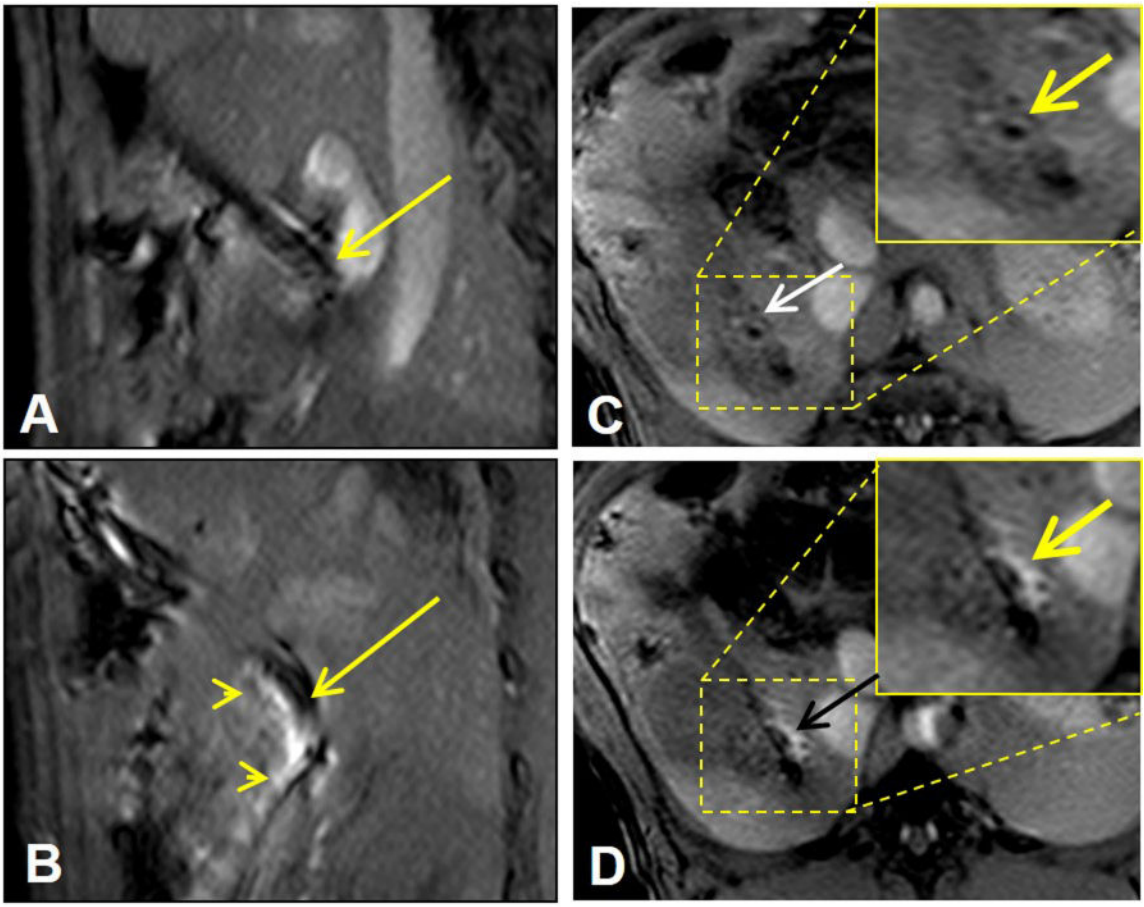


**Figure 3.**

MRI-guided local delivery of MGd/blue dye mixture into the pig CBD wall via the MR-compatible needle-integrated balloon system. **(A)** Sagittal T1WI clearly displays the needle in the CBD (arrow). **(B)** MRI-guided needle puncture into the CBD wall (arrow) and delivery of MGd into the tissue, which is shown as bright signal penetrating the CBD (arrowheads). **(C&D).** Cross-sectional view of the CBD wall before (arrow on C) and after local injection of MGd/blue dye, demonstrating the infiltration of MGd into the CBD wall and adjacent tissue (arrow on D).

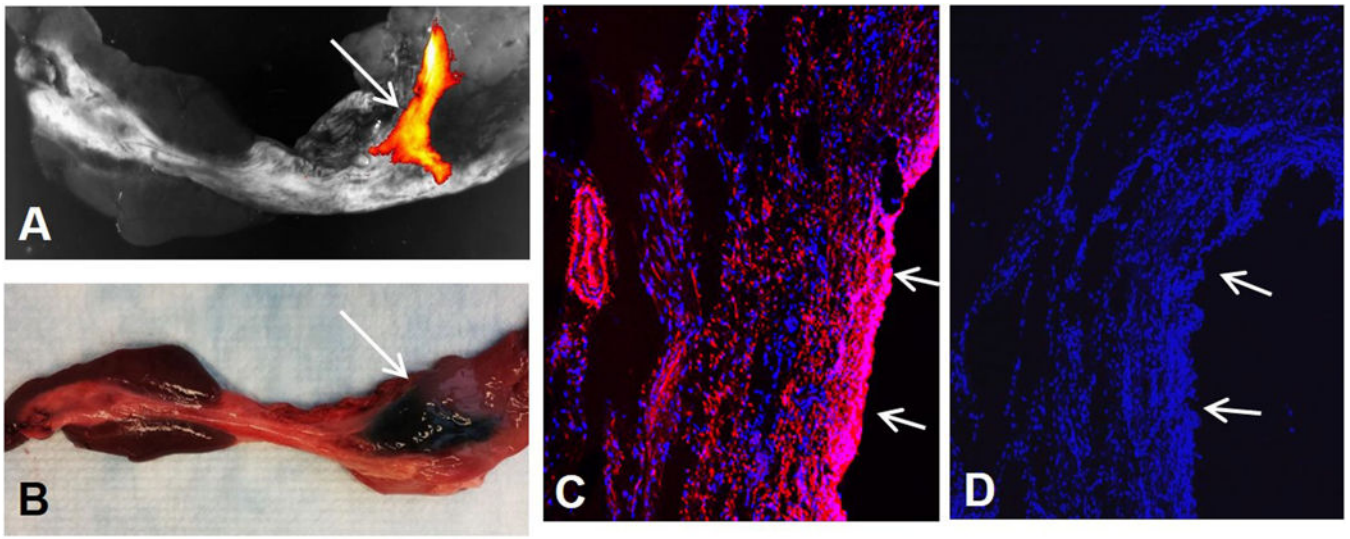


**Figure 4.**

(**A**) Optical imaging of the CBD delivered with MGd and trypan blue mixture, showing MGd-emitting fluorescence in the targeted CBD wall (arrow). (**B**) Representative gross specimen of the CBD, demonstrating the blue dye staining of the targeted CBD and surrounding tissue (arrow). (**C&D**) Confocal microscopy confirms the infiltration of MGd-emitting red fluorescence through the bile duct wall and adjacent tissue (**C**), which is not seen in the control bile duct without MGd injection (**D**). Arrows on C&D indicate epithelial layer of the CBDs.